nature genetics

Article

https://doi.org/10.1038/s41588-022-01254-1

Single-cell transcriptomic analysis of endometriosis

In the format provided by the authors and unedited

Supplementary Note

Single cell transcriptomic analysis of endometriosis

Fonseca*, Haro*, Wright*, Lin* *et al*

Additional Results

KRT10/ACTA2 Clusters

The *KRT10*/*ACTA2(1)* and *(2)* clusters were enriched for endometriosis tissues and depleted for eutopic endometrium, by contrast, nearly all the cells in *KRT10*/*ACTA2(3)* were derived from eutopic endometrium (Fig. 3b, c). *KRT10* expression is typical of stratified epithelium and is expressed by vaginal epithelium during development [1] with reported temporal fluctuations in endometrial expression throughout the menstrual cycle [2]. Since squamous epithelium is not typical of endometriosis or eutopic endometrium and *KRT10* expression was relatively low, we explored whether these cells may represent mesenchymal cell types. None of the 3 clusters exhibited a robust smooth muscle, endometrial-type stroma or mesenchymal marker signature (Supplementary Fig. 2a). *KRT10/ACTA2* clusters 1 and 2 exhibited a weak signature of proliferative endometrial-type stroma (in the case of cluster 2, without any detectable MME). Cluster 3 lowly expressed genes characteristic of secretory endometrial-type stroma; together these data suggest that these subsets may in fact represent less differentiated subsets of endometrial-type stroma. When we contrasted gene expression in *KRT10/ACTA2* cells from eutopic endometrium, endometriosis and endometriomas, eutopic endometrial *KRT10/ACTA2* cells were enriched for steroid hormone signaling (HSP90 chaperone cycle for steroid hormone receptors in the presence of ligand, adjusted $P = 3.3x10^{-6}$) and autophagy pathways (Supplementary Fig. 2b, c; Supplementary Tables 11 and 12). By contrast, the *KRT10/ACTA2* cells associated with endometriosis were enriched for secretory-associated pathways (such as peptide chain elongation, adjusted $P = 9.7x10^{-27}$) (Supplementary Fig. 2b).

Mesothelial cells proximal to endometriomas upregulate proinflammatory and stress response genes

Mesothelial cells are a specialized epithelial cell lining of the peritoneum, the pleurae, pericardium and ovary [3]. Re-clustering of mesothelial cells resulted in clusters driven largely by tissue type, although we noted heterogeneity in cell quality, with a tendency towards higher mitochondrial reads in endometrioma-associated cells (Supplementary Fig. 3a, b). Mesothelial cluster (1) (1,620 cells) comprised cells proximal to peritoneal lesions and comprised more differentiated mesothelia. Ovarian mesothelial cells, both from ovaries with and without endometrioma, dominated mesothelial cluster (2) (791 cells) and (3) (404 cells). Mesothelial cluster (2) was less differentiated than mesothelial cluster (1), with lower expression of keratins -7, 8 and 18, and mesothelial markers such as *CALB2, WT1* and *MSLN* (Figure 3b,b). Mesothelial cluster (3) were partially differentiated mesothelial cells with negligible keratin expression, low expression of *WT1* and *CALB2*, and modest *CD44* expression (Supplementary Fig. 3b, c). Mesothelial cells in specimens with no endometriosis detected upon pathologic review upregulated stress response pathways including ‘cytoprotection by HMOX1’

(adjusted P = 4.9 x 10^{-5}), a pathway for heme degradation, perhaps suggesting occult endometriosis existed in those specimens. Mesothelia associated with endometriomas upregulated *growth arrest and DNA damage inducible alpha* (*GADD45A*), likely an indicator of cellular responses to the hypoxic microenvironment imposed by the endometriotic cyst (Supplementary Fig. 3c-f; Supplementary Tables 15 and 16). Compared to endometriosis-free ovary tissues, mesothelium proximal to endometriomas overexpressed inflammatory modulators including *macrophage migration inhibitory factor* (*MIF*, $\log_2$ FC = 1.1, adjusted P = 6.7x10^{-136}), a proposed biomarker for endometriosis [4,5] (Supplementary Fig. 3e-f; Supplementary Tables 15 and 16). MIF can interact with multiple receptors (CD74/CD44, CXCR2, CXCR4, and CXCR7) [6]. *CD74* was expressed by endothelial cells, B-cells/plasma cells and myeloid cells; *CXCR4* was expressed by myeloid cells, T/NK cells and B-cells/plasma cells (Supplementary Fig. 3g). Expression of *CXCR2* and *ACKR3* (*CXCR7*) plus *CCL2* receptor *CCR2*, was not detected in any of the cell types surveyed. B-cells/plasma cells are enriched 2.6-fold in endometriomas (Figure 1f), and MIF is important for B-cell chemotaxis and B-cell survival and activation [7 8], raising the possibility that mesothelial cells proximal to an endometrioma contribute to the recruitment of B-cells.

Mesenchymal cells in endometriosis and control tissues

GAS5+ cells were the dominant mesenchymal cell type in unaffected ovaries. Four clusters of fibroblasts exhibited heterogeneous expression of canonical fibroblast markers (*DCN*, *THY1*, *CFD*), three clusters of C7-positive fibroblasts and two clusters of activated fibroblasts expressing *FAP, ITGB1, COL1A1* and *ACTA2* - one C7 positive, the other C7 negative (Fig. 5b). C7-positive fibroblast clusters (1) and (3) and C7-positive activated fibroblasts were overrepresented in ovarian tissue adjacent to endometriomas. Two PDGFRA+ clusters - the Fibro(4) and C7 Fibroblast cluster (2), plus the C7-negative activated fibroblast cluster, were exclusively comprised of cells from peritoneal endometriosis specimens. Both these clusters expressed extracellular matrix and immune modulator *Coiled-Coil Domain Containing 80* (*CCDC80*)[33]. We verified that mesenchymal markers but not in epithelial markers were expressed by mesenchymal clusters (Supplementary Fig. 4a). We noted evidence of coordinated transcriptional signatures in endometrial-type epithelium and stroma, which was most pronounced in ectopic endometrium - with 9, 41 and 20 genes commonly upregulated in endometrial-type stroma and epithelium across eutopic endometrium, endometrioma and endometriosis, respectively (Supplementary Fig. 4b). Epithelial and stromal cells in endometriosis upregulated secretory genes (ribosomal proteins e.g. *RPL13A, RPS18*), whereas the same cell types in the context of endometrioma upregulated complement signaling pathways (*C3*, *C7*, *C1S*, *CFH;* Supplementary Fig. 4c) and genes involved in responses to the heme-laden cytotoxic and hypoxic microenvironment (*HMOX1, SOD2*), reflected also by a tendency for higher percentages of mitochondrial RNA in endometrioma samples (Supplementary Figs. 3b, 4b).

The cellular composition of deep and superficial peritoneal lesions

Eleven peritoneal lesions were categorized as deep infiltrating endometriosis and 12 were classified as superficial endometriosis, comprising a total of 69,131 individual cells. Within these 23 lesions, the abundance

of fibroblasts negatively correlated with the proportion of T/NKT cells (r=-0.95, P < 0.01, Pearson's correlation), B/Plasma cells (r=-0.60, P < 0.01, Pearson's correlation) and mast cells (r=-0.43, P < 0.05, Pearson's correlation) (Supplementary Fig. 5a). B/plasma cells, T/NKT and mast cells were modestly enriched in deep lesions, and endothelial cells, epithelial cells and fibroblasts were moderately enriched in superficial lesions (Supplementary Fig. 5b). To test whether these enrichments indicated that an overall cellular signature was associated with lesion subtype, we simulated a background data set based on the frequencies of the different cell types in the actual data and measured Euclidian distance between deep and superficial lesions, based on frequencies of all cell types (Supplementary Fig. 5c). Using this alternative approach there was no significant difference in the cellular composition of deep and superficial lesions (P = 0.85, compared to a background of 1,000 randomly generated data sets, *pnorm* R function using mean and standard deviation from background) (Supplementary Fig. 5d, e), suggesting that, when considering major cell types, there is no specific cellular signature associated with deep *versus* superficial lesions. Hemorrhage and fibrosis were also not associated with cellular composition (P = 0.53 and P = 0.40, respectively) (Supplementary Fig. 5f).

Supplementary Methods

Pathology

A protocol was created and implemented in the pathology laboratory to ensure collection of endometriosis samples from consented patients without risk of compromising the ability to provide clinical histopathologic diagnoses on resected tissue (Supplementary Fig. 6)

Supplementary Figure Legends

Supplementary Figure 1. Histologic and macroscopic features of lesions from the endometriosis cohort. (a) Images from surgeries during which the specimens were collected (not to scale). (b) Hematoxylin and eosin-stained sections of specimens profiled in this study. Scale bars (5mm) apply to all images shown in (b). Surgical and pathology images for specimens from Patient 9 are shown in Fig. 1b.

Supplementary Figure 2. *KRT10/ACTA2* cells in eutopic and ectopic endometrium. (a) Expression of mesenchymal, smooth muscle and endometrial-type stromal (proliferative and secretory) gene expression in KRT10/ACTA2 clusters. Mesenchymal and smooth muscle clusters from Fig. 2 are shown for context. (b) Pathway analysis, performed in Reactome, with p-values calculated based on a hypergeometric model and a Bonferroni correction applied. (c) Differential gene expression in the three clusters that comprise the *KRT10*/*ACTA2* subset, in the context of endometrioma, eutopic endometrium or extra-ovarian endometriosis (p value < 0.05 and $\log_2$ FC > 1), two-sided differential expression tests performed using MAST.

Supplementary Figure 3. The impact of endometriomas on ovarian mesothelial cells. (a, b) Quality metrics across mesothelial, endometrial-type epithelium and endometrial-type stroma clusters. (c) UMAP of mesothelial cell clusters, by major class (d) Feature UMAPs illustrating expression of genes overexpressed in endometriosis or endometrioma. (e) Differential gene expression in mesothelial cells adjacent to endometrioma compared to mesothelial cells in unaffected ovary (labeled genes are those where adjusted $P < 0.05$ and absolute log2 FC > 0.8). (f) Pathway analysis in mesothelial cells in the context of endometrioma, endometriosis, unaffected ovary or peritoneum without pathologic confirmation of endometriosis. Pathway analysis was performed using the Reactome R package, with p-values calculated based on a hypergeometric model and a Bonferroni correction applied. (g) Dotplot, expression of MIF and CCL2 receptors across all major cell types.

Supplementary Figure 4. Coordinated transcriptional responses of endometrial-type stroma and epithelium in eutopic endometrium, endometriosis and endometrioma. (a) Epithelial markers are not expressed by mesenchymal clusters and *vice versa*. (b) Heatmap, coordinated expression of genes in endometrial-type epithelium and stroma across eutopic endometrium, endometrioma and endometriosis. Ordering of columns are supervised, ordering of rows unsupervised and clustered using hierarchical clustering (method = complete). n, number of genes in each category; common denotes genes changing in both the epithelial and stromal compartments. (c) Pathway analysis for genes in each of the 3 groups in panel (b). Pathway analysis was performed using the Reactome R package, with p-values calculated based on a hypergeometric model and a Bonferroni correction applied.

Supplementary Figure 5. Molecular signatures of deep and superficial peritoneal endometriosis and testing for associations between cellular composition and clinical features of endometriosis. (a) Cellular components of peritoneal endometriosis, correlations between abundance of different cell types in each lesion. Significant associations from two-sided Pearson correlation tests – $^{1}p = 0.022$; $^{2}p = 0.044$; $^{3}p = 3.7x10^{-11}$; $^{4}p = 3.6x10^{-3}$; $^{5}p = 0.025$; $3.7x10^{-11}$; $^{6}p = 4.2x10^{-3}$; $^{7}p = 2.1x10^{-5}$; $^{8}p = 9.1x10^{-3}$; $^{9}p = 0.03$; $^{10}p = 5.8x10^{-3}$. SM, smooth muscle cells. The grey area represents the 95% confidence level interval for predictions from a linear model. (b) Proportional bar plot showing frequencies of major cell types in deep and superficial lesions, relative to the null distribution denoted in the Total row. (c) Euclidean distance between samples, compared to a simulated background distribution of 1000 random samples. Deep/superficial status, presence/absence of hemorrhage or fibrosis were all surveyed. Box and whisker plots, boxes denote the interquartile range, bar denotes median value. The limits of the whiskers represent 1.5 * IQR (interquartile range) and outlier values are indicated with individual dots. (d) Cell type composition of extra-ovarian endometriosis samples, (e) Schematic of the approach to compare Euclidian distances between samples, compared to a simulated background data set. (f) Cell type composition across the simulated data set.

Supplementary Figure 6. Pathology protocols for collecting endometriosis tissues for research

Supplementary References

1. Cunha, G. R. et al. Molecular mechanisms of development of the human fetal female reproductive tract. Differentiation. 97, 54–72 (2017).
2. Ponnampalam, A. P., Weston, G. C., Trajstman, A. C., Susil, B. & Rogers, P. A. W. Molecular classification of human endometrial cycle stages by transcriptional profiling. Mol. Hum. Reprod. 10, 879–893 (2004).
3. Auersperg, N., Wong, A. S., Choi, K. C., Kang, S. K. & Leung, P. C. Ovarian surface epithelium: biology, endocrinology, and pathology. Endocr. Rev. 22, 255–288 (2001).
4. Elbaradie, S. M. Y., Bakry, M. S. & Bosilah, A. H. Serum macrophage migration inhibition factor for diagnosing endometriosis and its severity: case-control study. BMC Womens Health 20, 189 (2020).
5. Morin, M. et al. Elevated levels of macrophage migration inhibitory factor in the peripheral blood of women with endometriosis. Fertil. Steril. 83, 865–872 (2005).
6. Noe, J. T. & Mitchell, R. A. MIF-Dependent Control of Tumor Immunity. Front. Immunol. 11, 609948 (2020).
7. Klasen, C. et al. MIF promotes B cell chemotaxis through the receptors CXCR4 and CD74 and ZAP-70 signaling. J. Immunol. 192, 5273–5284 (2014).
8. Gore, Y. et al. Macrophage migration inhibitory factor induces B cell survival by activation of a CD74-CD44 receptor complex. J. Biol. Chem. 283, 2784–2792 (2008).

Patient Number	Surgical Image				
1	Left ovary 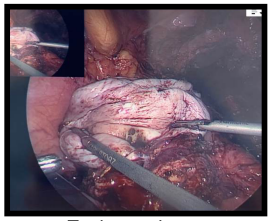				
2	Endometrioma 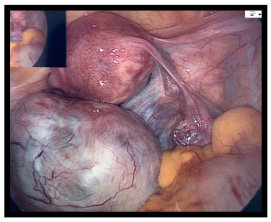	Posterior cul-de-sac 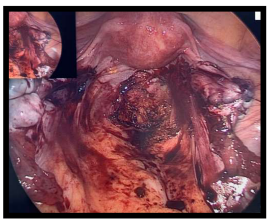			
4	Anterior cul-de-sac 1 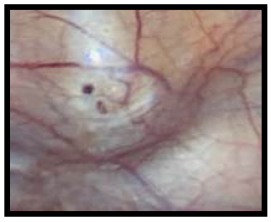	Anterior cul-de-sac 2 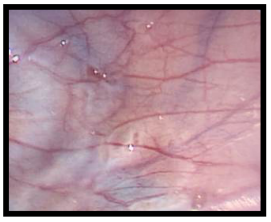	Posterior cul-de-sac 1 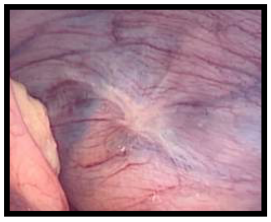	Posterior cul-de-sac 2 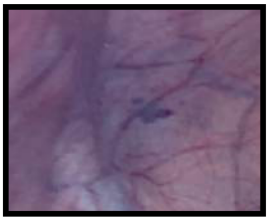	
5	Posterior cul-de-sac 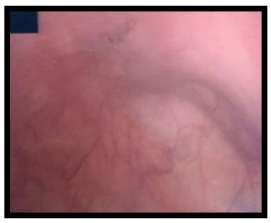				
7	Pelvic sidewall (R) & Uterosacral ligament (R) 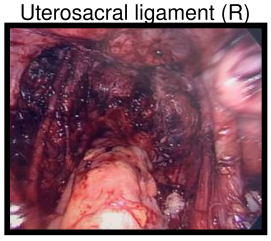	Pelvic sidewall (L) & Uterosacral ligament (L) 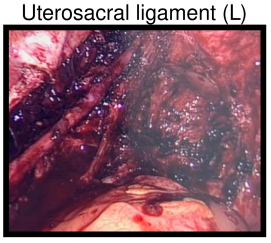	Anterior cul-de-sac 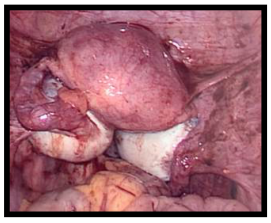		
8	Anterior cul-de-sac 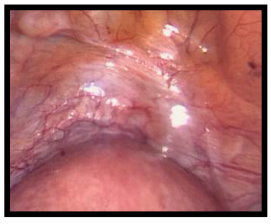	Pelvic sidewall (R) & Uterosacral ligament (L) 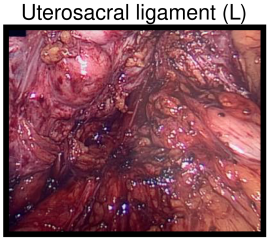	Rectal serosa 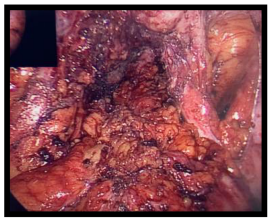		
10	Uterosacral ligament 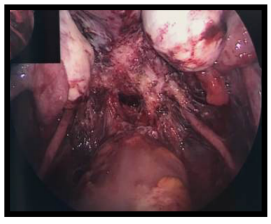	Bladder 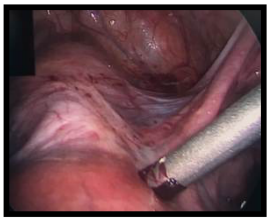	Pelvic sidewall (L) 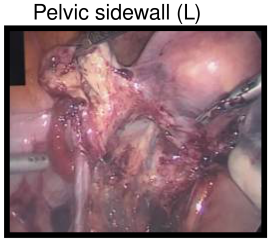		
11	Pelvic sidewall (L) 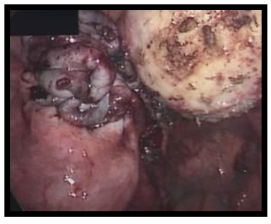				

Supplementary Fig. 1a part 1

Patient Number

Surgical Image

Supplementary Fig. 1a part 2

14

Ovary (R) & (L)

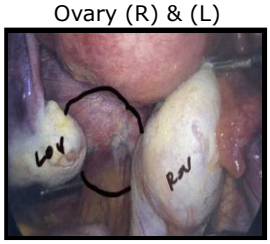

15

Ovary (R)

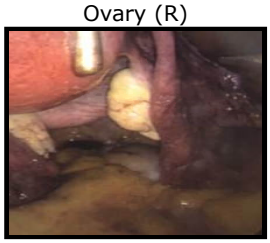

16

Ovarian fossa (L)

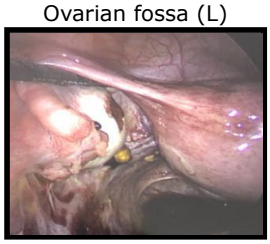

19

Endometrioma (L)

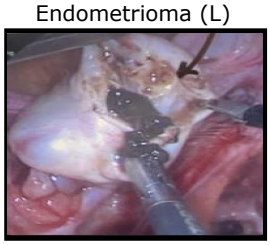

Ovarian fossa (R)

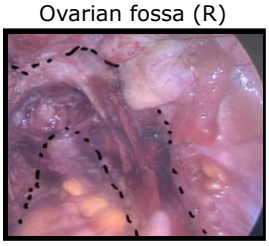

20

Uterosacral ligament (L) & (R)

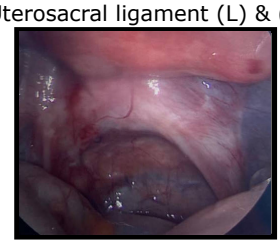

21

Ovarian fossa (L)

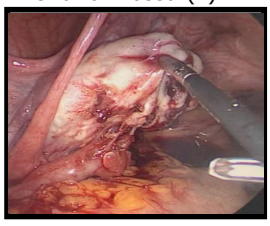

Uterosacral ligament (R)

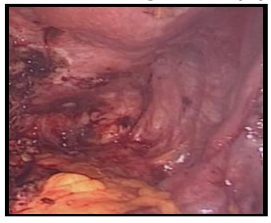

Anterior cul-de-sac

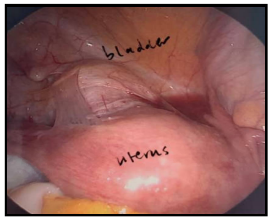

Posterior uterus

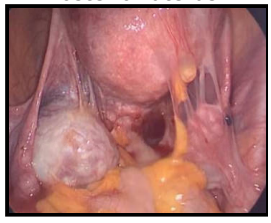

Patient Number

H&E Images

Supplementary Fig. 1b part 1

1

Endometrioma(L)

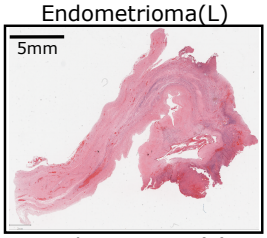

2

Endometrioma(L)

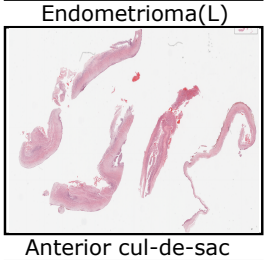

Endometrioma(R)

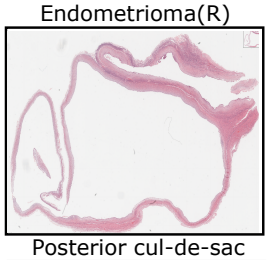

4

Anterior cul-de-sac

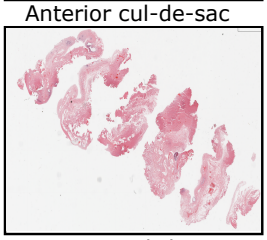

Posterior cul-de-sac

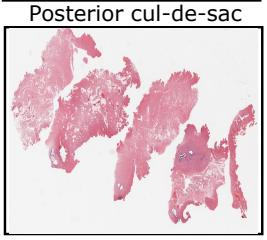

5

Posterior cul-de-sac

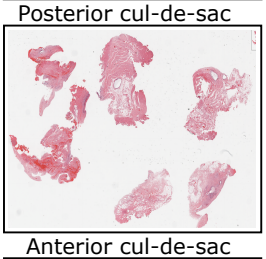

7

Anterior cul-de-sac

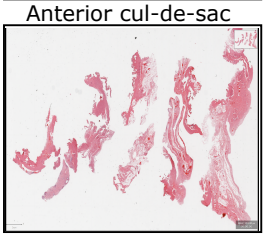

Pelvic side wall (L)

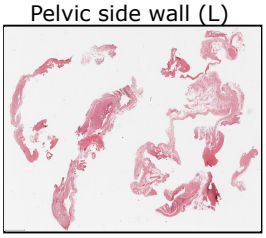

Pelvic side wall (R)

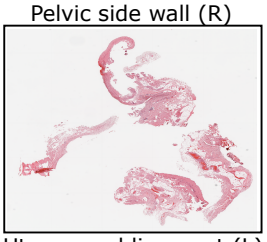

Uterosacral ligament (L)

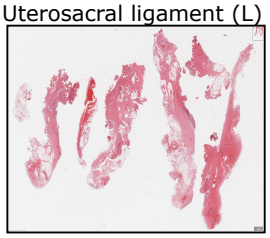

Uterosacral ligament (R)

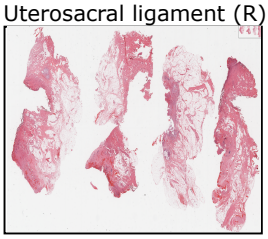

8

Anterior cul-de-sac

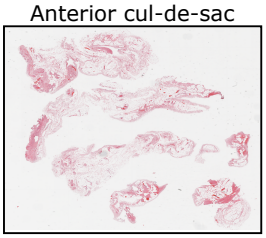

Pelvic side wall (R)

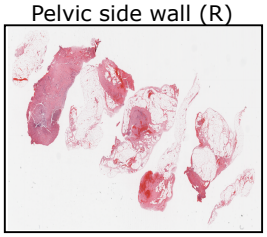

Uterosacral ligament (L)

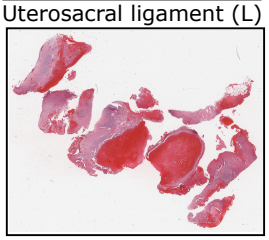

Rectal serosa

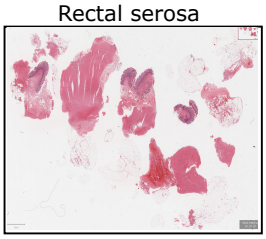

10

Bladder

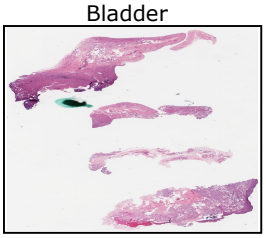

Pelvic side wall (L)

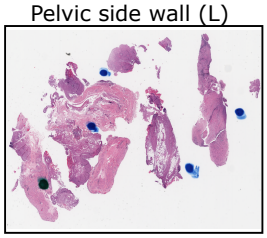

Pelvic side wall (R)

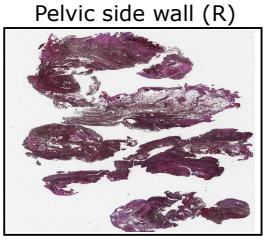

Uterosacral ligament (L)

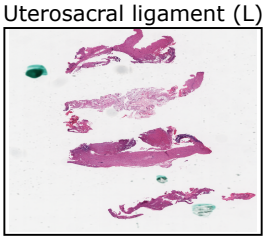

Uterosacral ligament (R)

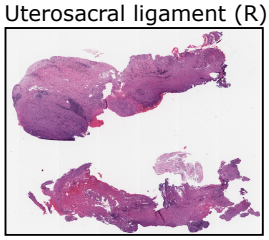

11

Endometrioma(L)

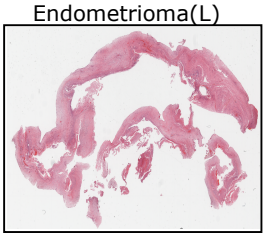

Pelvic side wall (L)

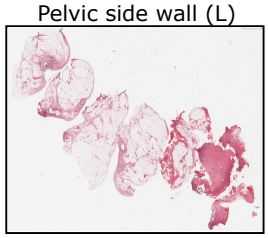

Patient Number

H&E Images

Supplementary Fig. 1b part 2

14

Ovary endometriosis (R)

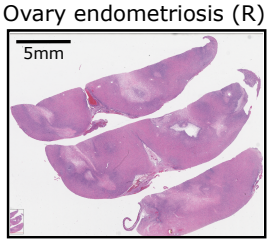

16

Ovarian fossa (L)

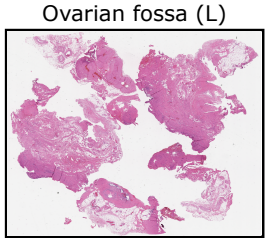

19

Endometrioma (L)

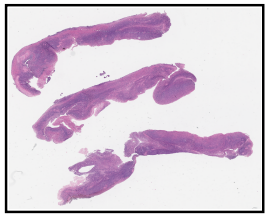

Ovarian fossa (R)

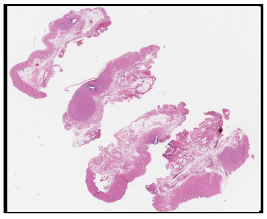

20

Uterosacral ligament deep (L)

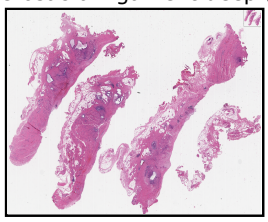

Uterosacral ligament superficial (L)

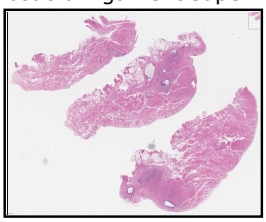

21

Rectum

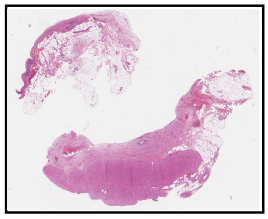

Uterosacral ligament (R)

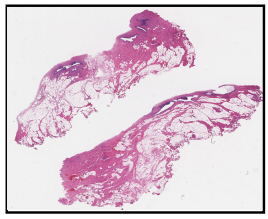

Anterior cul-de-sac

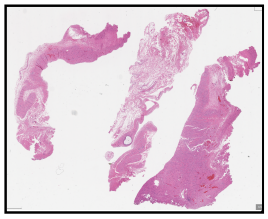

Posterior uterus

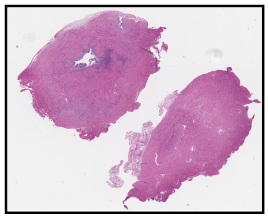

Ovarian fossa (L)

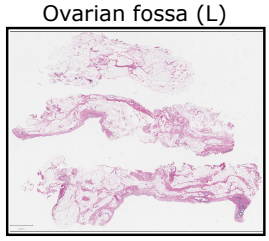

Supplementary Fig. 2

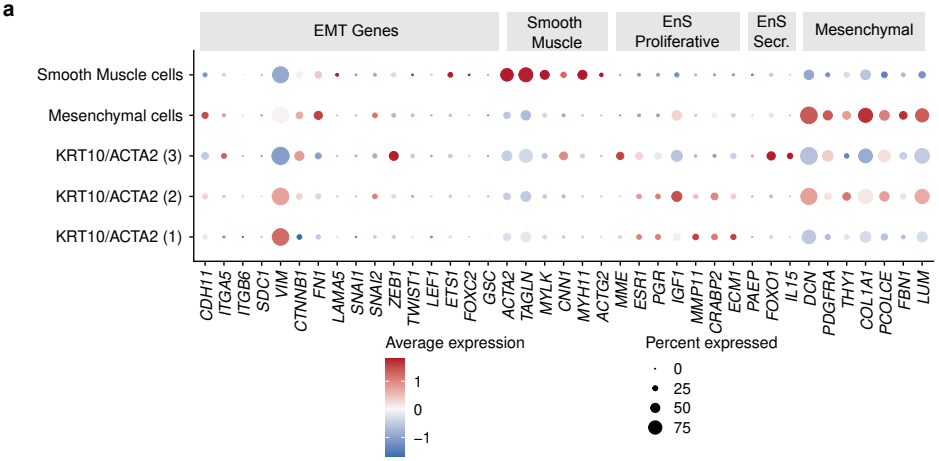

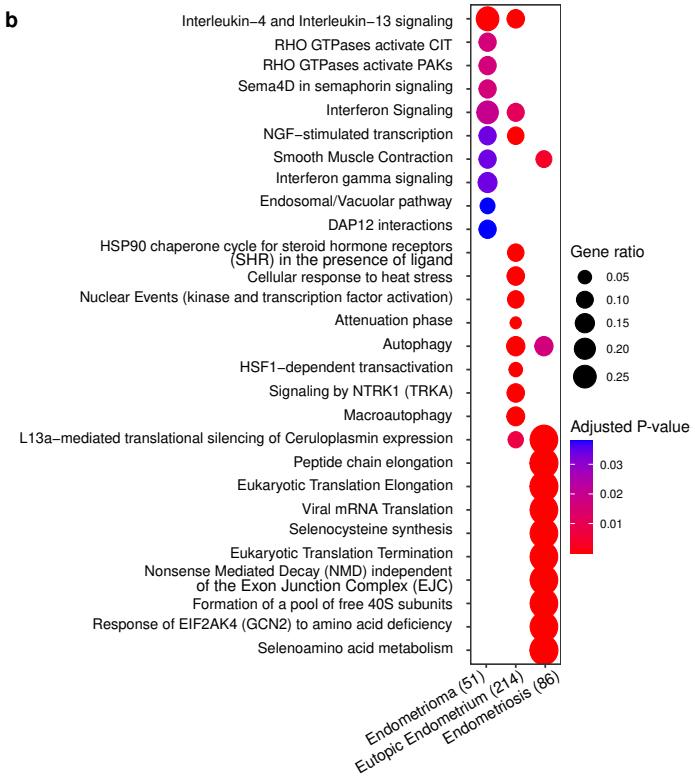

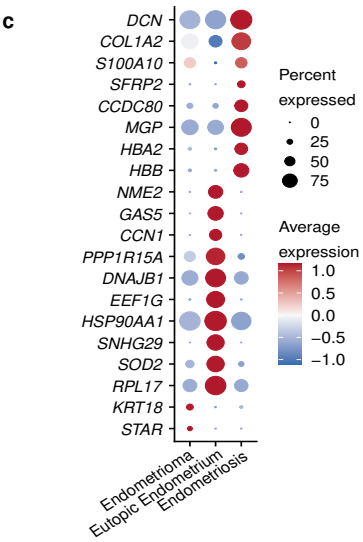

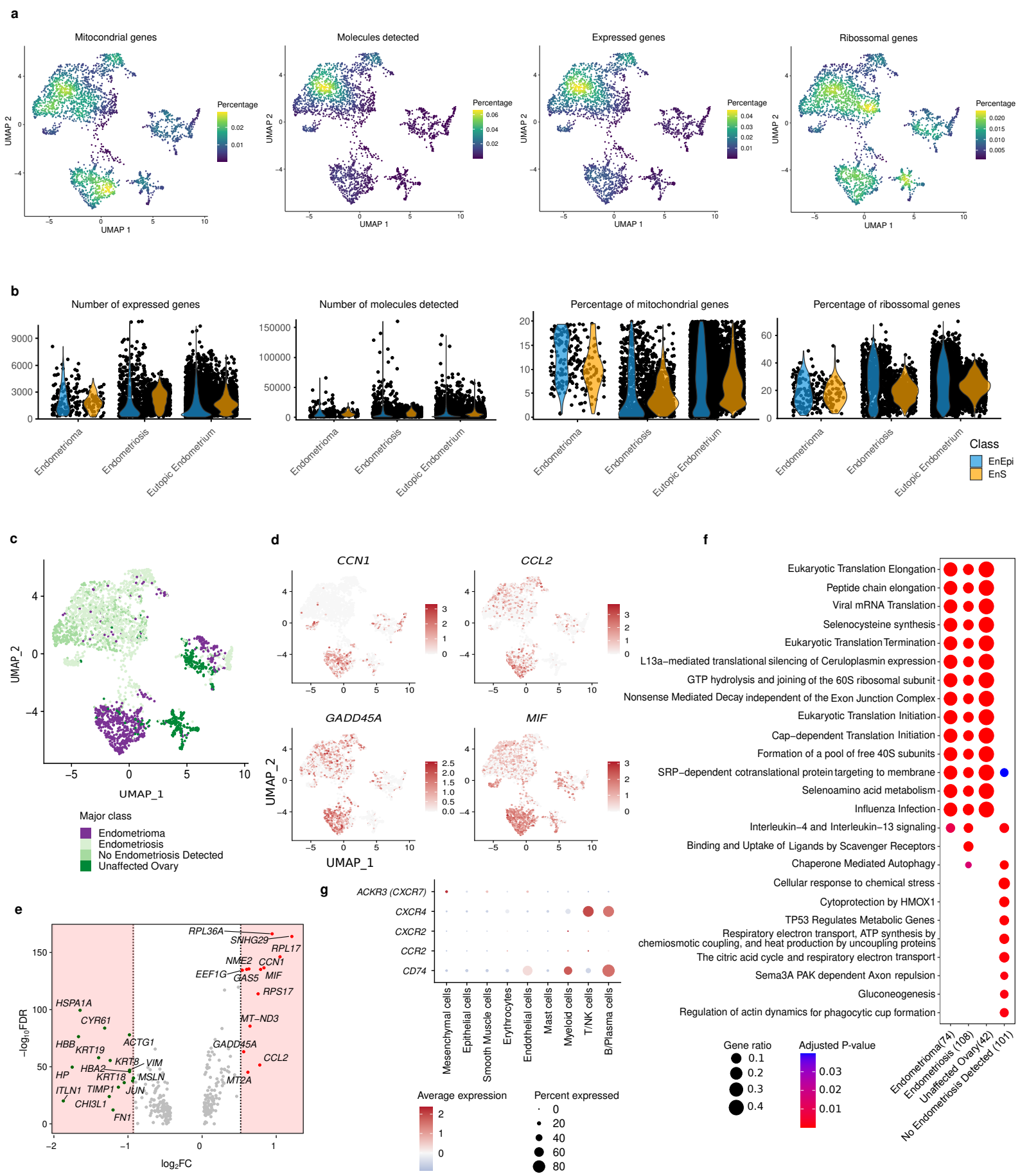

Supplementary Fig. 3

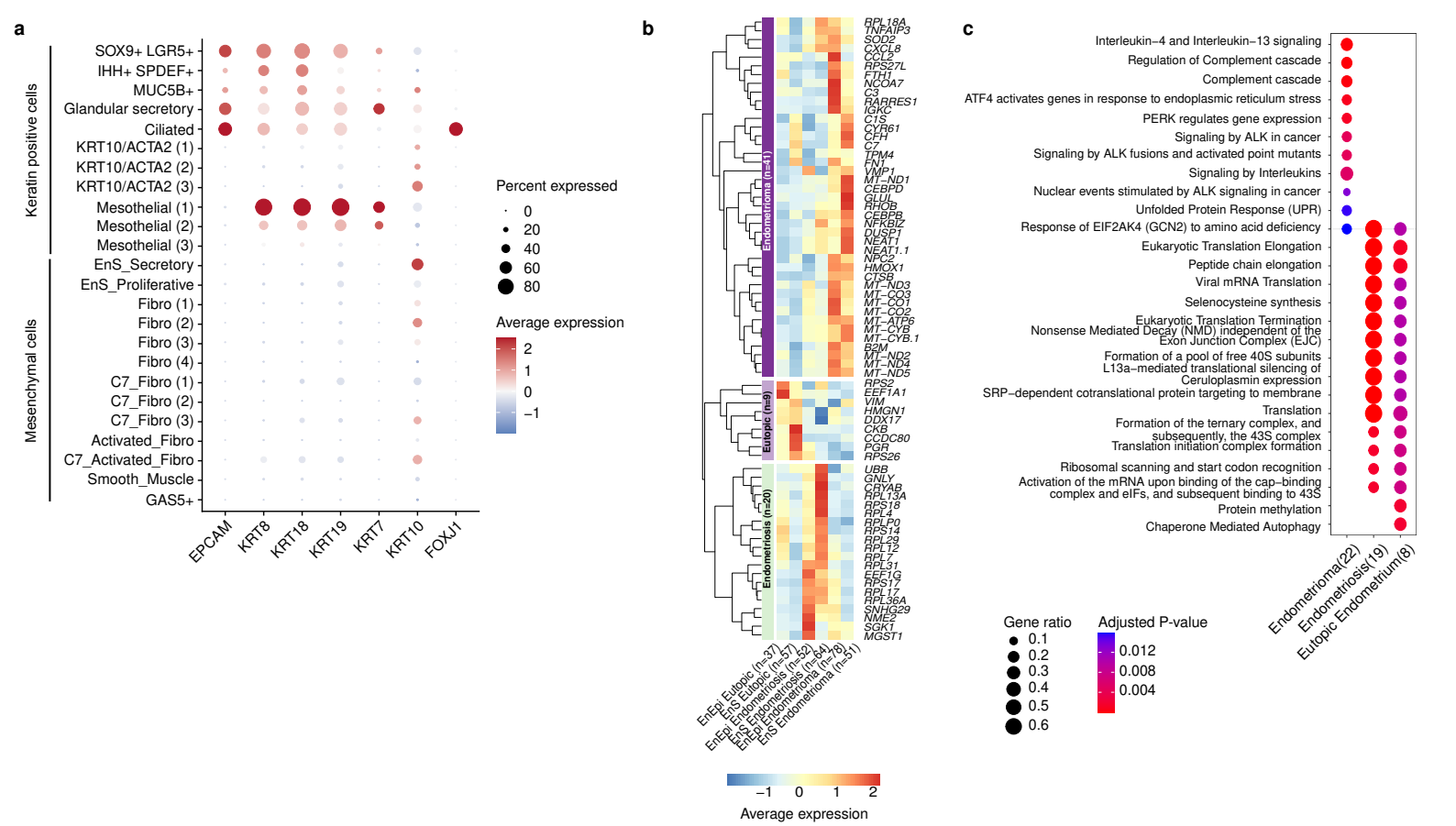

Supplementary Fig. 4

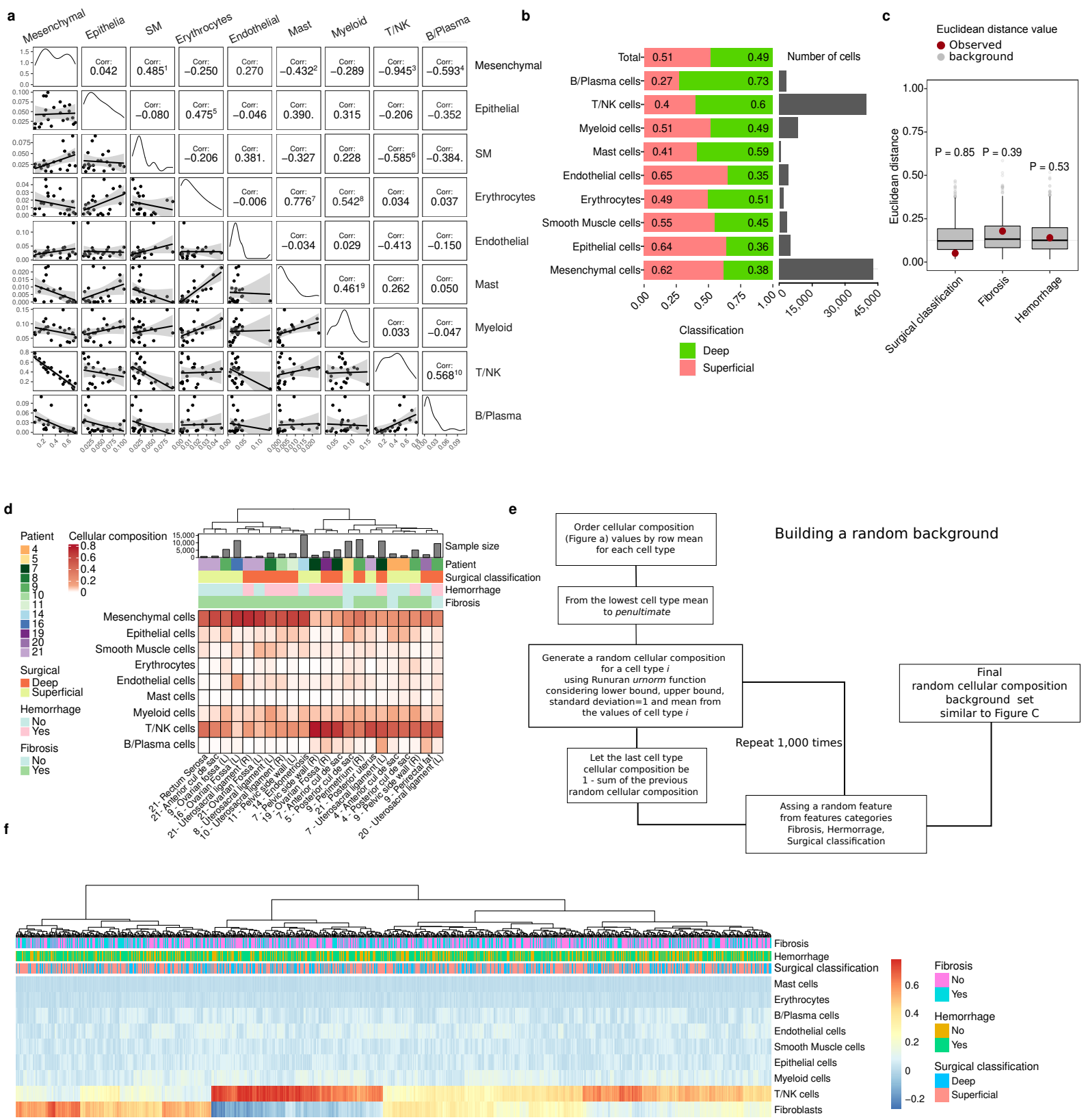

Supplementary Fig. 5

Supplementary Figure 6. Pathology protocols for collecting endometriosis tissues for research

Ovarian Endometrioma

- Serially section the ovarian cyst
- Randomly select multiple areas from the cyst wall including predominantly the inner lining to for research
- Aim to select 3 different areas if cyst is < 3 cm in largest dimension
- Aim to select 5 different areas if cyst is > 3 cm in largest dimension
- The remaining tissue is entirely submitted for permanent sections

Extra-ovarian Endometriosis (Superficial Peritoneal and Deep Infiltrating)

Patients undergoing surgery for recurrent endometriosis:

- Tissue fragment ≤ 1 cm: Bisect and submit half for research and half for permanent sections.
- Tissue fragment > 1 cm: Serially section and submit half of alternating sections for research and half for permanent sections.

Patients undergoing first surgery for endometriosis:

- Tissue fragment ≤ 1 cm: Submit all tissue for permanent sections. No tissue given for research.
- Tissue fragment >1 cm and grossly hemorrhagic area: submit half of hemorrhagic area for research and half for permanent sections. Likewise, the non-hemorrhagic areas are submitted half for research and half for permanent sections.
- Tissue fragment >1 cm and no grossly visible hemorrhagic area: Submit all tissue for permanent sections. No tissue given for research.

Extra-ovarian Endometriosis (Visceral)

For small biopsies, the same rules above as peritoneal/soft tissue apply.

For larger resections, for example colon:

- Open and/or serially section the organ fresh to identify grossly abnormal areas (hemorrhagic, cystic, fibrotic)
- If only a few small foci are present, submit half of these areas for research and half for permanent sections
- If extensive areas are grossly abnormal, randomly select abnormal tissue for research and permanent sections